Experimental Measurements and Numerical Simulation of Dense Spray at the Outlet of Pressure Swirl Injector

D. Ferrando*, C. S. Vegad, S. Idlahcen, A. Vandel, B. Renou, G. Godard, G. Cabot, J. B. Blaisot, B. Duret, J. Reveillon, F.X. Demoulin

CORIA-UMR 6614, Normandie University, CNRS-University and INSA of Rouen, Avenue de l'Université, BP 12, Saint-Étienne-du-Rouvray 76800, France
*Corresponding author: ferrandd@coria.fr

Abstract

N-heptane hollow cone spray of an industrial pressurized liquid swirl injector is investigated experimentally and numerically. The dense region of emerging spray near the injector orifice is the primary focus of this study. Atmospheric unconfined CORIA Rouen spray burner (CRSB) is adopted to atomize n-heptane. The burner comprises a hollow cone spray injector and an external annular passage to supply non-swirling co-flow air around the injector. The internal flow field of this injector is investigated in our previous work [1]. In this paper, the measurements and simulations are carried out for the dense spray of an external flow field. The overall spray behavior is characterized by microscopic shadowgraphy imaging. The droplet size and velocity at different axial and radial downstream locations are measured using phase Doppler anemometry (PDA). The numerical work is focused on simulating the near field region using a Volume of Fluid (VoF) based method in a Large Eddy Simulation (LES) framework. Simulations are carried out using the `OpenFOAM` library, in particular, the incompressible multiphase solver `interFoam`. The liquid-gas interface and their curvature are then analyzed by the method proposed by [2] obtaining the Sauter mean diameter (SMD) and droplet size distribution of the spray. This analysis has been further developed [3] allowing us to compute the velocity joint distribution of the droplets characterizing better the formed spray at an early stage of the atomization process. The results showed a favorable agreement between measured and simulated droplet size and velocity.

Keywords

Simplex atomizer, PDA, Volume of Fluid, SMD, dense spray

Introduction

Near field regions are the locations where the primary breakup of continuous liquid stream is taking place in the gaseous medium. These regions are optically dense as they carry droplets, ligaments and complex liquid structures. They offer information concerning the formation of droplets. In other words, an early stage of atomization process has a significant impact on the dispersed phase. The present attempt is to conduct experimental measurements in the near nozzle field using state-of-the-art spray diagnostic techniques and to perform numerical simulations for these dense spray regions using the Volume of Fluid (VoF) method in the LES framework.

Multiple approaches have been carried out to image the dense sprays. Unfortunately, there is no single technique available that can offer all the information required to describe the entire spray. The choice of diagnostic technique is based on the region under investigation. The overall behaviour of the flow field near the injector orifice can be imaged by means of microscopic shadowgraphy [4]. Since it is line-of-sight imaging, the images may contain an out-of-focus spray regime.

However, high contrast images of two-phase flows can be achieved with the use of laser imaging techniques. For example, the liquid core that is surrounded by a massive number of droplets can be captured by ballistic imaging [5, 6]. When the laser-illuminated detection technique, i.e.,

Mie scattering, is applied to a dense spray, non-physical spray information in terms of artifacts takes part in the final images. In this technique, the direct reflection of incident laser light at the liquid-air interface of non-spherical liquid structures creates signals that are strong enough to saturate the camera sensor. On the other hand, the multiple scattering of incident light introduces the blurring effect that reduces the visibility of spray structures.
One of the potential methods to reduce multiple scattering is by structured illumination [7]. This technique uses a spatially modulated laser sheet intensity to differentiate direct and multiple scattering. Further, contrary to the Mie detection, the laser-induced fluorescence (LIF) detection technique provides high contrast images of dense spray. LIF is recommended for detailed analysis of ligaments, droplets and other liquid structures present at the beginning of atomization process [10, 11, 15, 16]. A review of different techniques to image principal spray regions is given in [12] and that for dense zones refer [13, 14].
The current approach is organized as follows. The n-heptane hollow cone spray is imaged using microscopic shadowgraphy in the near nozzle field. The grid points for the PDA measurements are estimated from the observations of shadowgraphy data. The droplet size and velocity distributions are obtained from the curvature analysis of numerically obtained initial spray [2]. In the end, numerically obtained droplet size and velocity are compared with measured values.

Experimental Setup and Technique

The experimental test facility is schematically presented in Fig. 1. In the present study, the CORIA Rouen spray burner (CRSB) was adopted to carry out n-heptane atomization process. CRSB consists the fuel injection system and plenum. The fuel injector is located at the top of the injection system and opens into the chamber (Fig. 1). Injector is surrounded by a co-flow air stream guided through a convergent annular passage. The outer and inner diameters of annular passage at downstream end are 20 mm and 10 mm, respectively. While the upstream end is connected to the plenum that houses 18 radial vanes of zero-degree angle. The supplied air passes through the plenum is directed towards the radial vanes and finally enters the chamber. The purpose of providing radial vanes is to break large flow structures. Further details on burner geometry are available in [17, 18].
A cylindrical coordinate system is considered here. In Fig. 1, Z and R represent the axial and radial directions, respectively. The direction of arrow indicates the positive direction. The spray takes place towards the positive Z-direction. An industrial pressurized swirl injector (Danfoss make) of 80° hollow cone and 1.35 kg h^{-1} flow rate was used to atomize n-heptane fuel. The injector orifice diameter is 200 μm. The internal geometry of the injector is such that a portion of fuel pressure is utilized to form a rotating liquid film leading towards the orifice. While the remaining portion of fuel pressure is applied to force the liquid through an orifice as a conical sheet into the chamber. The chamber has a glass window fitted on each of the four sides. The chamber end faces the exhaust system to remove the fully atomized spray and thus avoid fogging within the chamber. In this way, and with co-flow air, liquid film formation on chamber walls can be avoided.
For all the experiments, n-heptane and co-flow air mass flow rates are 6 g s^{-1} and 0.28 g s^{-1}, respectively. N-heptane mass flow rate was regulated by Coriolis mass flow controller (Bronkhorst, CORI-FLOW, 0-2 g s^{-1}). The air mass flow rate was controlled by a thermal mass flow controller (Bronkhorst, EL-FLOW, 0-15 g s^{-1}). The K-type thermocouples were used to measure n-heptane (T1) and air (T2) temperatures. Their injection pressures were measured using the PT1 and PT2 pressure transducers (see Fig. 1).
A microscopic shadowgraphy was carried out at 25 kHz to capture the n-heptane hollow cone spray starting from the nozzle orifice up to droplet formation zones. Since the primary breakup is within 1.5 mm axial distance, it is recommended to use a microscope [11]. This was accomplished by using a long-distance microscope (LDM, QM-100, Questar) with a CMOS camera (1280 $\times$ 800 pixel^2 resolution, Phantom V2512). The complete imaging was within 5.32 $\times$ 3.33 mm^2 field of view at 4.16 μm per pixel optical magnification.

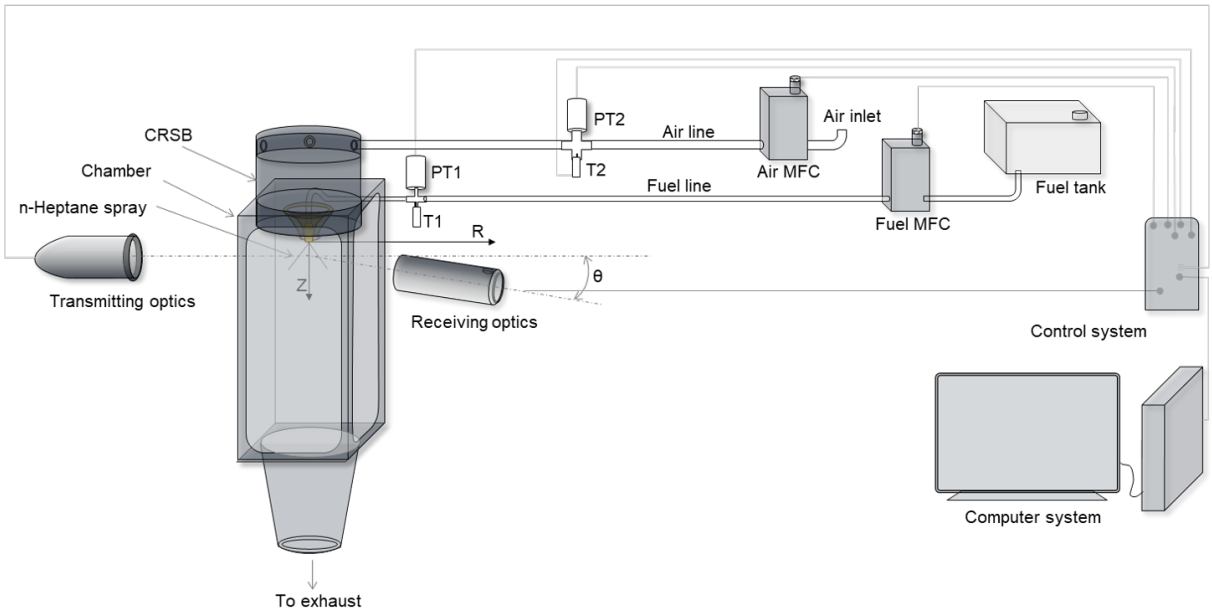

Figure 1. Schematic of an overall arrangement of experimental test facility. The position of transmitter and receiver probes of PDA correspond to spray are shown. In the figure— 1 and 2 refers n-heptane and air; MFC, mass flow controller; T, thermocouple; PT, pressure transducer; Z and R represent axial and radial directions.

A two-color phase Doppler anemometry (PDA) system (Dantec make) measured droplet size and velocity at near field locations. Figure 1 demonstrates the position of transmitter and receiver units. The green (514.5 nm) and blue (488 nm) argon laser beams are utilized for measurements. Each beam diameter is 2.2 mm and beam spacing is 38 mm. Focal lengths of transmission and receiver lenses are 350 mm and 310 mm, respectively. Beam crossing foams a probe volume of 0.148 $\times$ 0.148 $\times$ 3.10 mm^3. The receiver probe was set at θ = 70° off-axis angle in front scattering mode. It is close to Brewster angle for n-heptane (refractive index, n = 1.392). In this way, the effect of trajectory ambiguity can be reduced while collecting reflected and refracted light by the receiver probe. The acquisition was limited by 30 seconds or 1,20,000 droplets to achieve convergent statistics. The measurement was carried out from Z = 1 mm downstream of the injector orifice. It is shown in the following discussion that the validation rate close to the orifice is lower because of the presence of non-spherical spray structures and maybe the change in morphology of droplets.

Numerical Modelling Setup

The numerical modelling of this particular simplex swirl atomizer was done in [1] measuring the internal geometry of the injector to be able to define the numerical domain. Following a Volume of Fluid (VoF) based approach, the internal flow was computed. Nevertheless, due to the low mesh resolution above the nozzle, the atomization process was not properly captured; thus, a second simulation was carried out on a smaller but more refined numerical domain beginning on the nozzle orifice. To setup this last simulation, the velocity vector $\mathbf{u}$ and the liquid volume fraction α were extracted from the first simulation and mapped into the more refined one obtaining better qualitative agreement with experimental results. In this work, more recent results from the atomization process simulation are shown alongside the interface-curvature analysis of the liquid structures to compute, numerically, the diameter distribution of the spray.
The numerical simulation is performed with the `OpenFoam v6` toolbox following previous work. In particular, the `interFoam` solver, which is an incompressible VoF based solver that is able to capture the liquid-gas interface through a sharpening interface term on the liquid volume fraction advection equation, is used. A LES framework has been followed and the WALE sub-grid scale model has been retained from the internal simulation (see [1]). In contrast with the previous work, where the liquid sheet had a constant liquid sheet thickness, in this work, the liquid

sheet thickness varies on time and space due to fluctuations produced inside of the atomizer. The velocity and liquid volume fraction mapping from the internal to the external simulation is done through a Dirichlet time-varying boundary condition. Both side patches of the domain are periodic boundary conditions, atmospheric pressure is set at the outlet and no-slip boundary condition has been set at the wall. As it was done on the internal simulation, second order schemes are used on time and on space. The computational grid and boundary conditions used are shown on Fig. 2. A refinement zone is made in a hollow cone shape following the spray cone angle by [18] in order to capture better the liquid-gas interface. Refinement zone cell size is setup to dx = 1.2 μm with a total of 88 $\times$ 10^6 computational cells on this 45° sector domain.

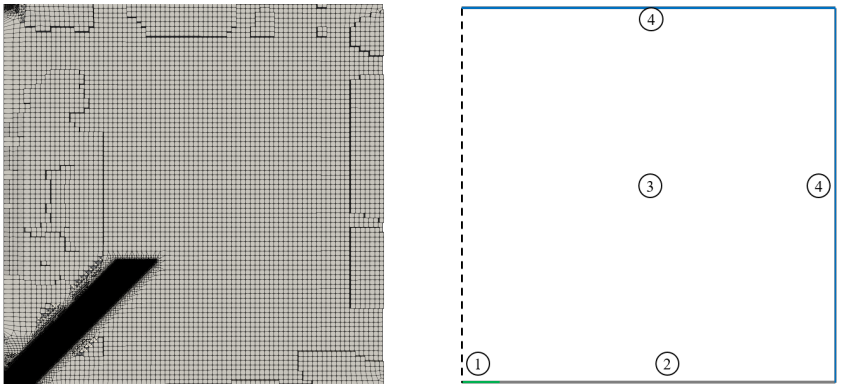

Figure 2. On the left, central slice of the numerical grid. A hollow cone refinement zone is performed to capture better atomization process and liquid-gas interface. On the right, simulation boundary condition. 1: Inlet (time varying mapping from internal simulation); 2: Wall (no-slip); 3: Side patches (periodic); 4: Outlet (atmospheric pressure).

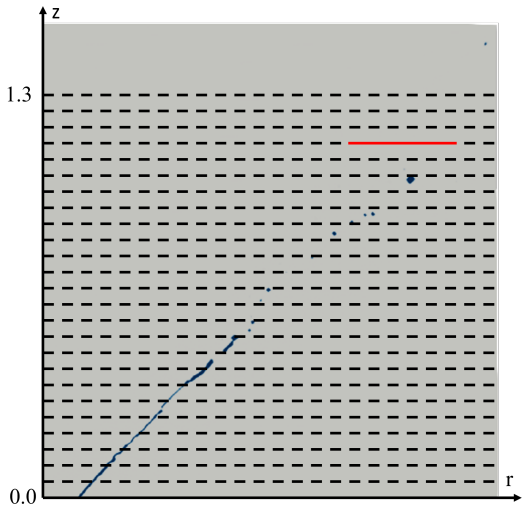

Figure 3. Liquid volume fraction contour. Dashed black lines represents the planes where the surface interface and liquid volume fraction are stored to compute the equivalent SMD. The red line represent the zone where the probes are setup in order to calculate the DSD.

In addition to previous work, the spray produced by the simplex swirl atomizer has been characterized through the interface-curvature analysis proposed by [2] and further developed in [3]. Several measurement planes are set up into the numerical domain (see Fig. 3) which measure the surface interface flux $\varphi\Sigma = (\mathbf{u}\cdot\mathbf{n})|\nabla\alpha|$ and the liquid volume fraction flux $\varphi\alpha = (\mathbf{u}\cdot\mathbf{n})\alpha$. Those quantities are integrated over the total area of the planes and on time giving us the total surface interface and liquid volume that go through those planes. Therefore, an equivalent Sauter Mean Diameter (SMD) or D_{32} could be defined even for non-spherical liquid structures as:

$$D_{32}(S) = 6\frac{\int_T \iint_S (\alpha \boldsymbol{u} \cdot \boldsymbol{n} ds)dt}{\int_T \iint_S (\Sigma \boldsymbol{u} \cdot \boldsymbol{n} ds)dt} \quad (1)$$

It is computed as a function of the axial coordinate to see the evolution of the breakup phenomena and determine where the continuous liquid sheet is breaking up into smaller liquid structures and turning into the final spray.
Furthermore, an additional zone of measurements is defined upstream and it is shown by a red line in Fig. 3. The zone is fulfilled with probes that store the curvature $\kappa = \nabla \cdot (\nabla\alpha/|\nabla\alpha|)$, the surface interface flux $\varphi\Sigma$ and the velocity $\mathbf{u}$ on the face of the cells each computational time step. The droplet diameter on each probe can be calculated as $D_\kappa = 4/\kappa$. Furthermore, the number of droplets crossing the probes zone are the ratio between the total surface interface $S = \int_T \iint_S (\Sigma \boldsymbol{u} \cdot \boldsymbol{n} ds)dt$ by the droplet surface for a given diameter $n_\kappa = S_\kappa/(\pi D_k^2)$. Thus, the droplet size distribution (DSD) can be reconstructed at the measurement zone. In addiction, since the velocity vector is known, the joint velocity distribution is also computed in a similar way.

Results and Discussion

As discussed earlier, the spray topology of n-heptane hollow cone spray for 0.28 g s^{-1} and 8.1 bar injection pressure was captured using microscopic shadowgraphy technique. The instantaneous image and averaged image (over 20 images) are shown in Fig. 4. The perturbations formed in the nozzle are grown in the outer part and can be seen at the liquid-air interface in Fig. 4(a). The magnitudes of sheet breakup distance and cone angle measured from the averaged image are in the order of 1 mm and 82° respectively. The primary objective of shadowgraphy was to estimate the locations for PDA measurements.

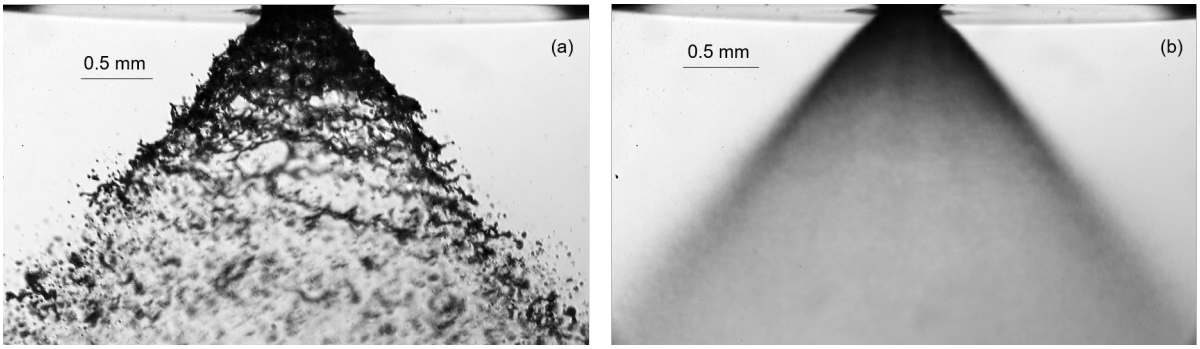

Figure 4. (a) Instantaneous shadowgraph image and (b) averaged over 20 images of n-heptane hollow cone spray at 0.28 g s^{-1} and 8.1 bar injection pressure.

Based on the observations made on shadowgraphy data, the PDA measurement started at an axial location Z = 1 mm for radial locations -2 mm $\leqslant R \leqslant$ 2 mm at 0.5 mm radial intervals. Similarly, the near-field measurements are performed by 1 mm axial increment up to Z = 5 mm, and 0.5 mm radial interval at each of these axial locations. To examine the spray symmetry, measurements are done on both sides of the central axis for all near field axial locations. Figure 5 shows the mean droplet diameter (D_{10}), and their axial (U) and tangential (V) mean velocities in the near-field region.
Larger droplets are found in the central region for a particular case at Z = 1 mm. This is because the presence of large liquid structures changes their topology as they evolve in R- and Z-direction. This can be noted from the validation contour line in Fig. 5(a), where spherical validation for 1 mm below nozzle is $\leqslant$ 70%. Even at this location, the data rate and droplet count (not shown here) are the lowest compared to other locations. Moving further down in the central region, for Z = 2 to 5 mm, the validation rate increased to ∼85%, and droplet diameter reduced from 10 μm to 6 μm. The reason could be that the smaller droplets coming from inner

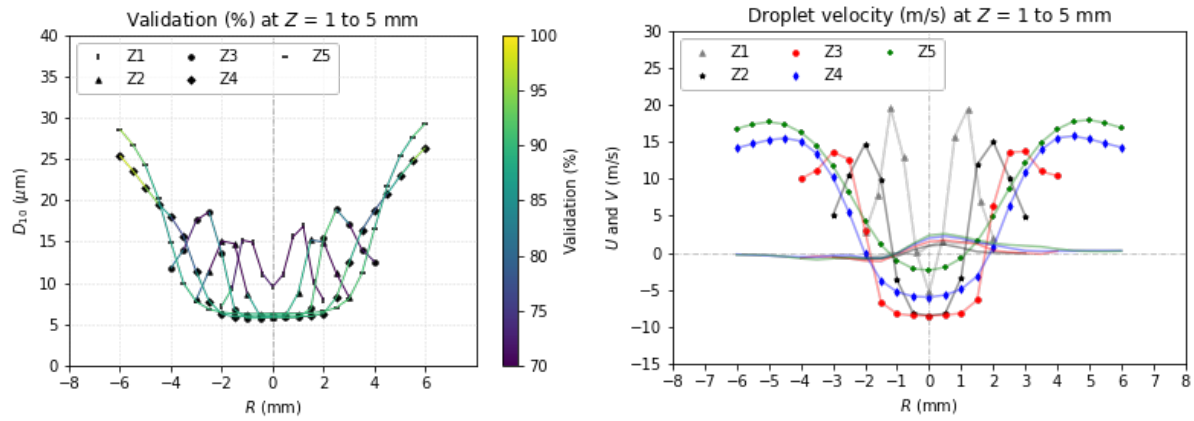

Figure 5. The measure droplet mean diameter (D10) along with the spherical validation (on left). The axial (U) and tangential (V) velocities measured by PDA in the near field regions (on right).

circulation zones are moving upward with negative axial velocity. One can notice the negative axial velocity (U) in Fig. 5(b). The tangential velocity (V) at the central part is in the order of 2 m s^{-1} and nearly 0 m s^{-1} at the outer zone. For convenience, in the present study, the inner and outer zones are defined as droplets having negative and positive axial velocities.
At the spray wall, defined as $Z \approx R$, the largest D_{10} and U are observed for Z = 1 to 3 mm. However, for Z = 4 and 5 mm, D_{10} is seen to be increased with R even beyond spray wall, see Fig. 5(a). Indeed, larger droplets exist at radially outward distances from the spray wall but with a reduced data rate. The axial velocity in the outer region increases with radial distance up to $Z \approx R$, and then decreases as it exhibits high radial velocity (not shown here).

Figure 6. Simulation iso-surface $\alpha = 0.5$ for two different time steps.

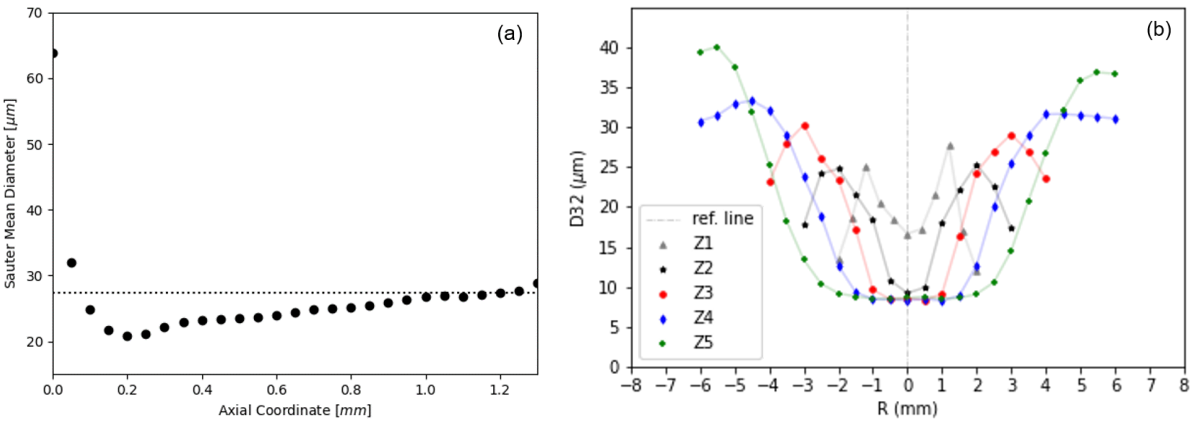

Figure 7. (a) Equivalent SMD evolution as a function of the axial coordinate (Z) on the numerical simulation following Eq. (1). (b) SMD calculated from the PDA measurements at various radial locations (R) in the close vicinity of injector.

The numerical simulation results are presented in Fig. 6. It shows the $\alpha = 0.5$ iso-surface for two different time steps. It is to be noted in Fig. 6 that the breakup of a liquid sheet takes place within a short axial location forming various ligaments. A close agreement in terms of spray

topology for both the results is worth noticing. Further, the length scale of numerically obtained liquid structures is in line with those captured by experiments (Fig. 4(a)). This is explained next. The equivalent SMD computed by Eq. (1) is plotted as a function of the axial coordinate (Z) in Fig. 7(a), and SMD obtained from PDA experiments for different R and Z is shown in Fig. 7(b). In Fig. 7(a), SMD at the nozzle orifice is maximum and equivalent to the sheet thickness. It is expected because the SMD calculations start on the basis of a hollow cone sheet. In Fig. 7(a), equivalent SMD decreases with radial locations up to Z = 0.2 mm. This happens due to the breakup of the continuous liquid sheet. Such sheet breakup results in the formation of verities of ligaments and droplets and thus increases the surface interfaces. The axial distance $Z = 0.2$ mm is the point where SMD reaches its lowest value, and no longer continuous liquid flow can be seen from this point. The primary breakup of a liquid sheet can be considered at this axial distance. From Z = 0.2 mm to the end of the refinement zones, the SMD value increases, which is similar to what was noticed in the present experimental results and previous study [18]. This effect is due to the fact that some small droplets do not follow the spray cone angle and leave the refinement zone. Consequently, the liquid volume fraction becomes diffuse, and the liquid-gas interface is no longer captured.

The magnitude of SMD becomes almost constant after the refinement zone. It is shown by a horizontal dotted line in Fig. 7(a). This SMD value, $\sim$28 μm, is close to the SMD measured at Z = R = 3 mm, as observed in Fig. 7(b). Before claiming the validation for this location, it is useful to compare the droplet size distribution (DSD) and axial velocity distribution obtained from numerical simulations and experimental measurements. In Fig. 8(a), simulated and measured DSD is presented. The y-axis represents the ratio of integrated values of droplet count divided by their magnitude. The black-filled bars are numerically obtained diameters, D, and solids stepped lines are measured diameters. Interestingly, and as discussed above, simulated DSD at R = Z = 1.2 mm is found to be in promising agreement with the DSD measured at R = Z = 3 mm. A possible reason may be the existence of spherical droplets (high validation) at this location compared to the upstream locations. In case of axial velocity distribution, the simulated value is higher than the measured at R = Z = 3 mm (Fig. 8(b)) but when it is compared at R = Z = 1 mm the shape and magnitude of the distribution looks more in agreement with numerical results. However, the obtained numerical velocity us still overestimated compared with experiments.

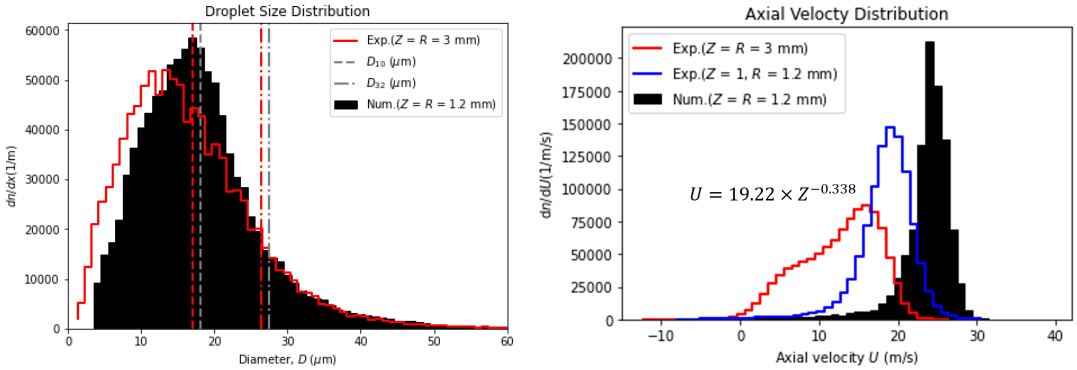

Figure 8. (a) comparison of simulated DSD with those obtained by PDA measurements in the near-field locations (Z = R = 3 mm) from the injector orifice. The vertical dashed and dash-dot lines are D_{10} and D_{32} respectively. Black color lines correspond to numerical work (Z = R = 1.2 mm). (b) Axial velocity distribution for both studies.

Summary

In this paper, n-heptane hollow cone spray of pressure swirl injector is numerically simulated and experimentally measured. The primary focus is to characterize the spray from curvature analysis in the near nozzle regions and compare the numerical results with the measurements in the close vicinity of an injector. The spray topology and liquid structures obtained from simulations are found to be in line with those observed in shadowgraphy imaging data. The

equivalent SMD and simulated DSD at R = Z = 1.2 mm are in reasonably close to the values measured at R = Z = 3 mm. However, this is not the case for axial velocity comparison. Further simulations should be performed to get closer to the measured axial velocity.

References

[1] Ferrando, D., Belmar-Gil, M., Palanti, L., Carreres, M., Cervelló-Sanz, D., Demoulin, F.-X., Renou, B., Duret, B., Reveillon, J., Aug. 29 - Sept 2. 2021, 15th Triennial International Conference on Liquid Atomization and Spray Systems.

[2] Palanti, L., Puggelli, S., Langone, L., Andreini, A., Reveillon, J., Duret, B., Demoulin, F.X., 2021, *International Journal of Multiphase Flows*, 147.

[3] Ferrando, D., Palanti, L., Demoulin, F.-X., Duret, B., Reveillon, J., Aug. 29 - Sept 2. 2021, 15th Triennial International Conference on Liquid Atomization and Spray Systems.

[4] Crua, C.; Heikal, M.R.; Gold, M.R. Microscopic imaging of the initial stage of diesel spray formation. *Fuel* 2015, 157, 140–150.

[5] Linne, M.A.; Paciaroni, M.; Berrocal, E.; Sedarsky, D. Ballistic imaging of liquid breakup processes in dense sprays. *Proc. Combust. Inst*. 2009, 32 II, 2147–2161.

[6] Idlahcen, S.; Rozé, C.; Méès, L.; Girasole, T.; Blaisot, J.B. Sub-picosecond ballistic imaging of a liquid jet. Exp. Fluids 2012, 52, 289–298

[7] Berrocal, E.; Kristensson, E.; Richter, M.; Linne, M.; Aldén, M. Multiple scattering suppression in planar laser imaging of dense sprays by means of structured illumination. *At. Sprays*. 2010, 20, 133–139,

[8] Wang, Y.; Liu, X.; Im, K.S.; Lee, W.K.; Wang, J.; Fezzaa, K.; Hung, D.L.S.; Winkelman, J.R. Ultrafast X-ray study of dense-liquid-jet flow dynamics using structure-tracking velocimetry. *Nat. Phys*. 2008, 4, 305–309

[9] Zhang, X.; Moon, S.; Gao, J.; Dufresne, E.M.; Fezzaa, K.; Wang, J. Experimental study on the effect of nozzle hole-to-hole angle on the near-field spray of diesel injector using fast X-ray phase-contrast imaging. *Fuel* 2016, 185, 142–150

[10] Berrocal, E.; Kristensson, E.; Zigan, L. Light sheet fluorescence microscopic imaging for high-resolution visualization of spray dynamics. *Int. J. Spray Combust. Dyn*. 2018, 10, 86–98,

[11] Durst, A.; Wensing, M.; Berrocal, E. Light sheet fluorescence microscopic imaging for the primary breakup of diesel and gasoline sprays with real-world fuels. *Appl. Opt.* 2018, 57, 2704

[12] Fansler, T.D.; Parrish, S.E. Spray measurement technology: A review. *Meas. Sci. Technol.* 2015, 26,

[13] Linne, M. Imaging in the optically dense regions of a spray: A review of developing techniques. *Prog. Energy Combust. Sci.* 2013, 39, 403–440,

[14] Coghe, A.; Cossali, G.E. Quantitative optical techniques for dense sprays investigation: A survey. *Opt. Lasers Eng.* 2012, 50, 46–56,

[15] Berrocal, E.; Conrad, C.; Püls, J.; Arnold, C.L.; Wensing, M.; Linne, M.; Miranda, M. Two-photon fluorescence laser sheet imaging for high contrast visualization of atomizing sprays. OSA Contin. 2019, 2, 983.

[16] Guénot, D.; Svendsen, K.; Björklund Svensson, J.; Ekerfelt, H.; Persson, A.; Lundh, O.; Berrocal, E. Simultaneous laser-driven x-ray and two-photon fluorescence imaging of atomizing sprays. Optica 2020, 7, 131.

[17] Cordier, M.; Vandel, A.; Cabot, G.; Renou, B.; Boukhalfa, A.M. Laser-induced spark ignition of premixed confined swirled flames. Combust. Sci. Technol. 2013, 185, 379–407.

[18] Verdier, A.; Marrero Santiago, J.; Vandel, A.; Godard, G.; Cabot, G.; Renou, B. Local extinction mechanisms analysis of spray jet flame using high speed diagnostics. Combust. Flame 2018, 193, 440–452.